ACS APPLIED MATERIALS & INTERFACES

Research Article

www.acsami.org

Facile Fabrication of a Well-Ordered Porous Cu-Doped SnO_2 Thin Film for H_2S Sensing

Shumin Zhang, Pingping Zhang, Yun Wang, Yanyun Ma, Jun Zhong, and Xuhui Sun*

Institute of Functional Nano & Soft Materials (FUNSOM), Jiangsu Key Laboratory for Carbon-Based Functional Materials & Devices, and Collaborative Innovation Center of Suzhou Nano Science & Technology, Soochow University, Suzhou, Jiangsu 215123, China

Supporting Information

ABSTRACT: Well-ordered Cu-doped and undoped SnO_2 porous thin films with large specific surface areas have been fabricated on a desired substrate using a self-assembled soft template combined with simple physical cosputtering deposition. The Cu-doped SnO_2 porous film gas sensor shows a significant enhancement in its sensing performance, including a high sensitivity, selectivity, and a fast response and recovery time. The sensitivity of the Cu-doped SnO_2 porous sensor is 1 order of magnitude higher than that of the undoped SnO_2 sensor, with average response and recovery times to 100 ppm of H_2S of ~10.1 and ~42.4 s, respectively, at the optimal operating temperature of 180 °C. The well-defined porous sensors fabricated by the method also exhibit high reproducibility because of the accurately controlled fabrication process. The facile process can be easily extended to the fabrication of other semiconductor oxide gas sensors with easy doping and multilayer porous nanostructure for practical sensing applications.

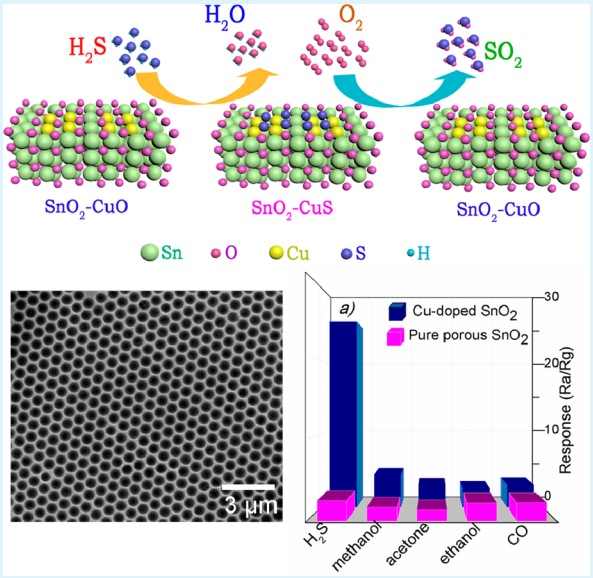

KEYWORDS: *gas sensor, metal oxide, porous film, doping, SnO_2, H_2S*

INTRODUCTION

Semiconducting oxide material-based gas sensors have been developed for a variety of applications such as industrial emission control, civil life, medical diagnosis, and environmental monitoring,[1−10] because of their irreplaceable advantageous features, such as high sensitivity, small physical size, low cost, and simplicity of fabrication. The gas sensing characteristics such as gas sensitivity, response time, selectivity, stability, and reproducibility are greatly influenced by the surface area, donor density, agglomeration, porosity, presence of catalysts, and sensing temperature of the sensing oxide materials. To achieve high-performance sensors, the synthesis process is one of the crucial factors for controlling the sensing properties of the final metal oxide, especially with respect to sensitivity and long-term stability.[11] Therefore, one major challenge in the improvement of gas sensors is to develop the facile approach to synthesize new functional materials, especially with well-defined structure and properties. Porous thin film materials with high surface-to-volume ratios are particularly promising in sensor fabrication. In addition, porous materials with defined nanostructural properties offer further advantages compared to conventional gas-sensing materials. Wet chemical methods for synthesizing porous thin films of metal oxides that allow the production of tailored and stabilized nanoparticles prior to their assembly in films have been developed, resulting in high sensitivity and reasonable stability.[12] However, the reproducibility of the sensing films prepared by wet methods is generally poor[13] because the structural parameters are difficult to control by conventional synthesis methods, such as the sol−gel process, and they are interdependent (e.g., grain size, grain interconnectivity, pore size, and pore architecture). Conventional physical deposition of metal oxide films such as sputtering deposition can improve the control over both material properties and film structural parameters but cannot generate the pores in the film. Here we report a method for preparing a well-ordered nanoporous metal oxide film by simple sputtering deposition using a self-assembly film of polystyrene spheres as a soft template.

Hydrogen sulfide (H_2S) is a toxic and inflammable gas, produced in sewage plants, coal mines, and oil and natural gas

Received: May 6, 2014
Accepted: August 12, 2014
Published: August 12, 2014

industries.[14] A wide variety of metal oxides have been studied for the detection of low concentrations of H_2S. Among these, SnO_2 films in which Cu is incorporated are the most promising for detecting H_2S.[15−19] The Cu element was dispersed either in the form of islands or as a continuous layer on the surface of the SnO_2 film yielded an improvement, with a reasonably strong sensor response to H_2S.[16,20,21]

In this paper, efforts have been made to prepare sensor structures via incorporation of Cu in the porous SnO_2 thin film by cosputtering deposition, which shows the enhancement in response to H_2S detection. The undoped and doped SnO_2 films have been fabricated by sputtering deposition combined with the soft template technique, in which the pore size and homogeneity of the film thickness can be precisely controlled, resulting in controllable sensing performance. The fabrication process is very simple and easy for practical applications. Such two-dimensional porous films created by the process developed in this work could be promising candidates for the other gas sensors.

EXPERIMENTAL SECTION

An aqueous suspension of 500 nm diameter polystyrene (PS) beads (2 wt %) was used to prepare the self-assembled closely packed monolayer PS templates for the fabrication of metal oxide porous thin films. A 500 nm SiO_2 layered Si wafer was used as the substrate, and the dielectric SiO_2 layer electrically isolates the metal oxide sensing film from the Si substrate for the sensor measurement. Prior to spin-coating of the suspension on the SiO_2/Si substrate, the substrate was treated with O_2 plasma, which made the surface hydrophilic for better adhesion to PS beads. A drop of the PS bead suspension was then spin-coated onto the SiO_2/Si substrate and dried for 2 h in a drybox at room temperature for monolayer self-assembly. To adjust the pore size, reactive ion etching (RIE) was used for the PS template for 1−2 min with a power of RF 90W to etch the beads. After the RIE treatment, the SnO_2 thin film with a thickness of 100 nm was deposited onto the SiO_2/Si substrate by room-temperature RF sputtering using a SnO_2 target. A Cu-doped SnO_2 thin film was obtained by cosputtering Cu and SnO_2 targets simultaneously, and the dopant concentration was controlled by the rate of sputtering of Cu. After the deposition, the samples were subjected to an ultrasound treatment in toluene to wash out the PS beads and then calcined at 550 °C for 2 h to crystallize the films, resulting in the formation of thin films with closed−linked hollow pores on the substrate. The two Au and Ti electrodes with thicknesses of 50 and 5 nm, respectively, were deposited on the oxide thin film with a 100 μm gap that exposed the sensing material. The morphologies of all the samples were characterized by a scanning electron microscope (SEM) (Quanta 200 FEG, FEI). The crystallinity and phase of the films were investigated by X-ray diffraction (XRD) (Empyrean, PANalytical). X-ray photoelectron spectroscopy (XPS) (Kratos AXIS UltraDLD) was performed for further investigation of the chemical composition and chemical state of the films. Surface areas of the porous thin films were measured by the BET method using a middle-high pressure physical gas adsorption instrument (ASAP2050, Micromeritics). The gas sensing experiments were conducted on a home-built intelligent gas sensing analysis system. The analysis system offered substrate temperature control (from room temperature to 500 °C), which could adjust the sensor temperature with a precision of 1 °C. The sensor resistance and sensitivity were recorded and analyzed by the system in real time. The gas sensitivity (S) is designed as the R_a/R_g ratio, where R_g is the sensor resistance in a mixed target gas and air and R_a is that in air (base resistance). Response and recovery times are defined as the time needed for 90% of the total resistance change upon exposure to gas and air, respectively.

RESULTS AND DISCUSSION

To create porous nanostructures, the PS monolayer soft template self-assembled on a hydrophilic SiO_2/Si substrate. The spin-coating of an aqueous solution containing PS beads (500 nm in diameter) on the substrate with homogeneous monolayer close packing is shown in Figure 1a. The diameter

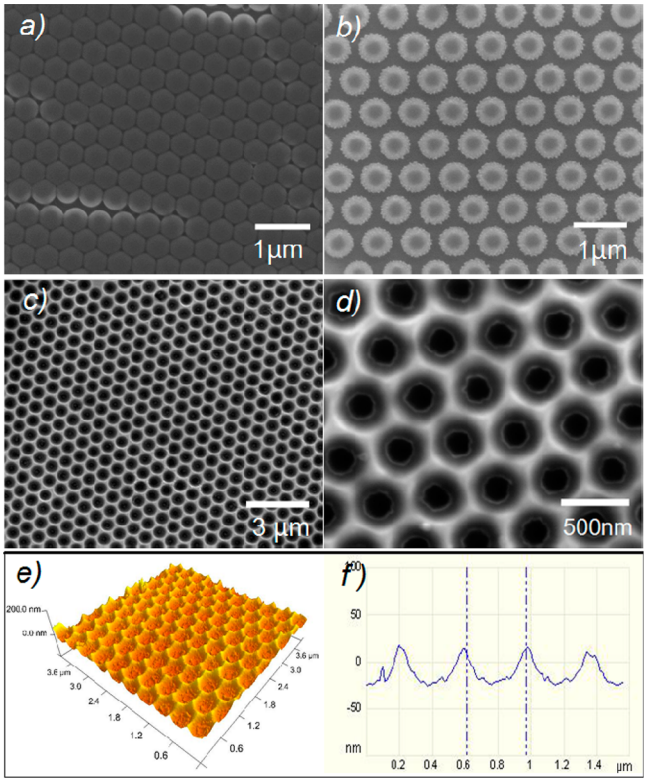

Figure 1. SEM images of (a) ordered PS monolayers on the SiO_2/Si substrate, (b) PS beads after RIE treatment, and (c and d) porous thin films at different magnifications. (e and f) AFM image and depth profile of the porous thin films, respectively.

of the PS beads was reduced by the oxygen plasma during the RIE process, which can accurately control the diameter of the PS beads by adjusting the power and the etching time of the oxygen plasma, as shown in Figure 1b. The oxygen plasma-etched PS bead monolayer was used as a soft mask to define the pattern of the porous film on the substrate. The pore size can be adjusted in this step by simply varying the O_2 etching time. The SnO_2 thin film was deposited onto the RIE-treated PS bead template by RF sputtering at room temperature and then annealed in the air at 550 °C to obtain the crystalline film. The PS beads can be washed out completely by an ultrasound treatment in toluene, according to the EDS spectrum (not shown) in which no obvious carbon peak can be scanned. Panels c and d of Figure 1 show the typical morphology of the nanostructured porous film on the substrate after annealing, which was fabricated from the PS bead (500 nm) template. The porous film exhibits uniform structure with hexagonally arranged pores approximately 200−300 nm in size. In addition, the depth of the pores in the thin film and three-dimensional surface topographic image can be gleaned from the atomic force microscopy (AFM) image (Figure 1e). Figure 1f shows AFM height scans. The data indicate that the surface of the film is relatively smooth and the depth of the pores is 75 nm on average.

The specific surface areas of the porous SnO_2 films have been investigated by a BET method. The N_2 adsorption−desorption isotherms are shown in Figure 1S of the Supporting Information, and the specific surface areas of the porous undoped SnO_2 and Cu-doped SnO_2 thin films in comparison with those of the plain SnO_2 film are summarized in Table 1.

Table 1. Specific BET Surface Areas of the Samples

form of the film	specific surface area (m^2/g)
plain SnO_2	4.7
undoped porous SnO_2	25.2
Cu-doped porous SnO_2	27.7

The porous films have surface areas much larger than that of the plain film, and Cu doping does not change the morphology or the corresponding surface area. The XRD data show that the as-deposited SnO_2 thin films are amorphous and become polycrystalline after the annealing treatment in air at 550 °C for 2 h. Figure 2S of the Supporting Information shows the XRD patterns of the SnO_2 porous film after a postdeposition annealing treatment and the Cu-doped SnO_2 porous film before and after the annealing treatment. All of the well-defined diffraction peaks in the spectrum of the undoped sample can be indexed as the tetragonal rutile structure of SnO_2 (JCPDS Card No. 77-0452). All the peaks in the XRD pattern of the Cu-doped porous thin film before annealing correspond to tetragonal structure of CuH_6O_6Sn (JCPDS Card No. 70-0117), indicating that the copper element is indeed doped into the tin oxide porous thin film. After the samples had been annealed, copper oxide and tin oxide separated from each other. The extra peaks marked as filled dots in the spectrum of the Cu-doped sample after annealing can be attributed to the monoclinic structure of CuO (JCPDS Card No. 89-2530). The XRD data indicate that the SnO_2 porous film upon thermal annealing is polycrystalline and the Cu dopant in the film exists in the form of CuO crystalline grains. The effect of Cu doping concentration on the sensing performance has been studied. Cu-doped thin film samples with different Cu doping percentages (2, 4, 6, and 8 wt %) were fabricated, and their corresponding sensing performance is shown in Figure 3S of the Supporting Information. The 6 wt % Cu-doped sample shows the best performance. Thus, the 6 wt % Cu-doped samples have been used in the following studies.

To further confirm the chemical states of Sn and Cu in the films, XPS analysis was performed on undoped and Cu-doped SnO_2 films, as shown in Figure 4S of the Supporting Information. Figure 4Sa shows the survey scan spectrum of the Cu-doped SnO_2 film, confirming the sample's composition of Sn, O, and Cu. The Si and C signals are from the Si substrate and carbon species absorbed on the surface, respectively. A common feature observed in the detail scan spectra of both undoped and Cu-doped SnO_2 films (Figure 4Sb) is the position of the main spin−orbit component of the Sn 3d peaks around 487 and 495 eV, which correspond to Sn $3d_{5/2}$ and Sn $3d_{3/2}$ core levels in SnO_2, respectively. In addition, the nature of the O 1s peak with a binding energy of 531 eV (not shown) supports the assignment and chemical stability of the SnO_2 films for all samples. The core level Cu 2p spectrum of the Cu-doped SnO_2 film (Figure 4Sc) shows a feature similar to that of Cu in CuO, and the observed binding energy is consistent with the value for Cu in CuO, which indicates that CuO has been successfully incorporated into the SnO_2 film. In addition, a clear shakeup feature of the Cu oxide around 940−945 eV is found, which further suggests that a CuO species is present.

The response transients of undoped and Cu-doped SnO_2 porous film sensors toward 100 ppm of H_2S gas balanced with air at 180 °C are shown in panels a and b of Figure 2,

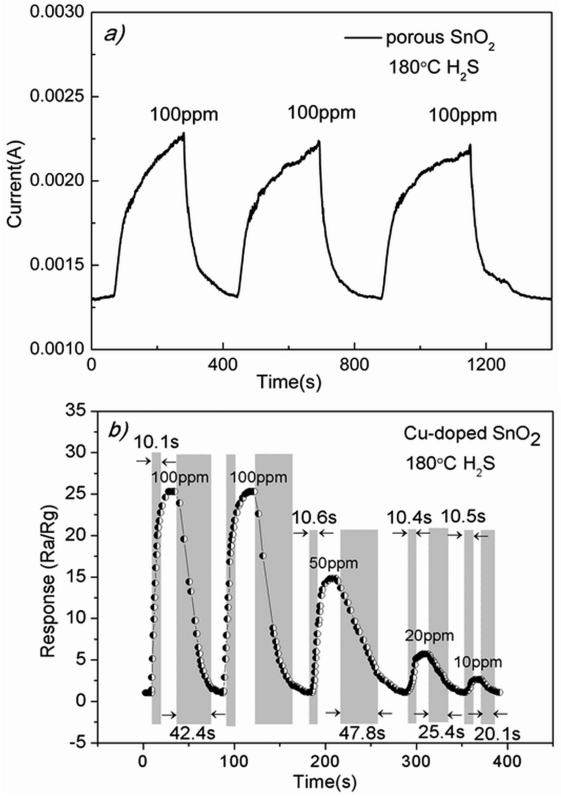

Figure 2. (a) Response curve of undoped porous SnO_2 film gas sensors to 100 ppm of H_2S. (b) Response curves of Cu-doped SnO_2 porous thin film gas sensors to different concentrations of H_2S gas at 180 °C.

respectively. The resistances of both undoped and Cu-doped SnO_2 sensors decreased rapidly upon the injection of H_2S and recovered with the exposure to air, exhibiting a typical n-type semiconductor sensing behavior. Compared with undoped porous SnO_2 thin film sensors, the Cu-doped SnO_2 porous thin film sensor exhibits a higher sensitivity and a shorter response and recovery time. The sensitivity of the Cu-doped SnO_2 sensor (R_a/R_g = 25.3) increases 1 order magnitude compared to that of the undoped sensor (R_a/R_g = 2.51) at 180 °C. The response and recovery times of the Cu-doped SnO_2 sensor are ∼10.1 and ∼42.4 s, respectively, on average, much shorter than those in the literature[17,22−25] and also shorter than those of the undoped sample with response and recovery times of 128 and 72 s, respectively. Because Cu doping does not increase the specific surface area according to BET measurements (Table 1), such high sensitivity and short response and recovery time of the Cu-doped SnO_2 sensor may be attributed to the Cu doping effect itself. The copper doping atoms have been turned into CuO in the SnO_2 porous film, which was confirmed by XRD and XPS data. When the sensors are exposed to H_2S, CuO is converted to CuS,[26] which is a metallic material with a good electrical conductivity, following reaction 1:

$$CuO(s) + H_2S(g) \rightarrow CuS(s) + H_2O(g) \quad (1)$$

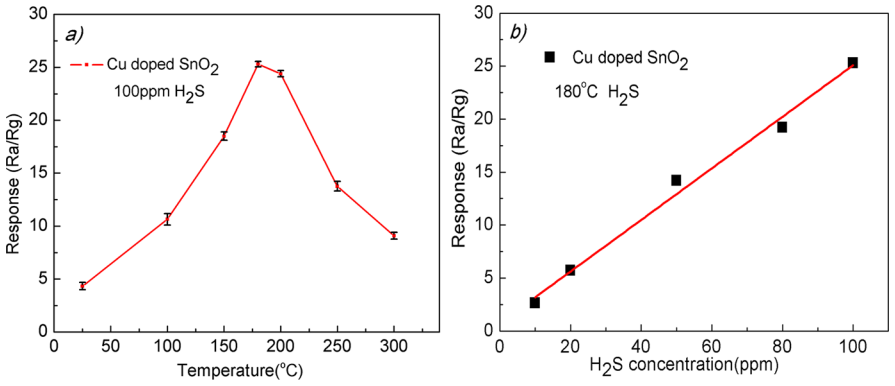

Figure 3. (a) Sensitivity of Cu-doped SnO_2 porous film sensors to 100 ppm of H_2S at different temperatures. (b) Sensitivity of Cu-doped SnO_2 porous film sensors to the concentration of H_2S that varied from 10 to 100 ppm at 180 °C.

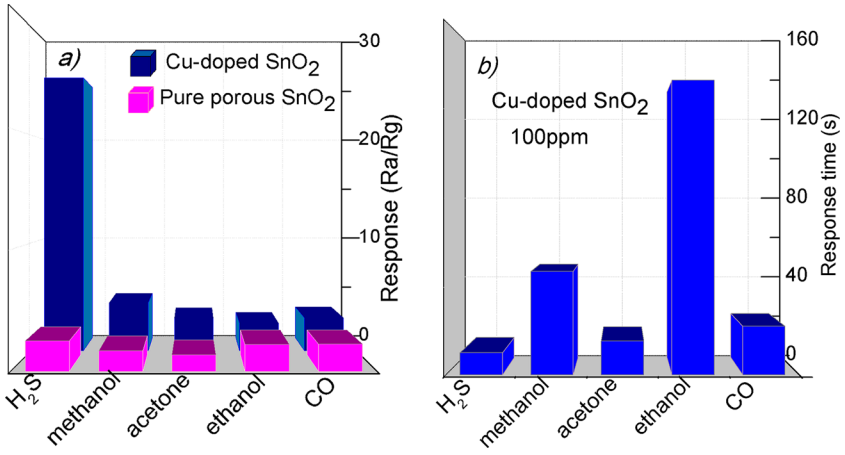

Figure 4. (a) Sensitivity of the undoped and Cu-doped SnO_2 porous film to different 100 ppm gases at 180 °C. (b) Comparison of response times of the Cu-doped SnO_2 porous film to different 100 ppm gases at 180 °C.

As a result, the electronic interaction between CuO and SnO_2 that gives rise to a very large electrical resistance of the sensor is disrupted upon exposure to the H_2S, leading to a drastic decrease in the electrical resistance and hence to the extremely high H_2S sensitivity. After H_2S gas is removed and air is introduced, CuS is converted back to CuO following reaction 2:

$$CuS(s) + {}^3/_2O_2(g) \rightarrow CuO(s) + SO_2(g) \quad (2)$$

Then the electronic interaction between CuO and SnO_2 is restored with the recovery of the original electrical resistance. A schematic illustration of the sensing mechanism of the Cu-doped SnO_2 thin film with respect to H_2S is shown in Figure 5S of the Supporting Information. In the following discussion, this sensing mechanism can also provide a reasonable explanation for the good selectivity of the Cu-doped SnO_2 sample to H_2S.

Sensing response characteristics of the Cu-doped SnO_2 sample over a temperature range from room temperature to 300 °C at 100 ppm of H_2S gas were also investigated and are shown in Figure 3. The response of the sensor increases initially with an increase in temperature, reaching a maximal value at an optimal temperature of 180 °C, and thereafter decreases. This phenomenon can be explained by the balance between the speed of chemical reaction and the speed of gas diffusion. At low temperatures, the sensitivity increases with an increase in reaction temperature. However, the diffusion speed of the target gas is accelerated at high temperatures. Thus, the two processes will tend to balance at a certain temperature at which the sensitivity of gas sensors becomes maximal.[27,28] In addition, the unstable CuS may also be responsible for the decrease in the response when the operating temperature is increased. It is reported that CuS can convert into Cu_2S when the temperature is further increased above 230 °C, and Cu_2S is a p-type semiconductor with a conductivity lower than that of CuS.[26,29] Even though the optimal temperature here is lower than 230 °C, the nanograins of CuS probably decrease the conversion temperature from CuS to Cu_2S. Hence, the response of the Cu-doped SnO_2 porous film shows the decrease with a further increase in the operating temperature. Figure 3b shows the sensitivities of the Cu-doped SnO_2 porous thin film sensor to different concentrations of H_2S in the range of 10−100 ppm at 180 °C. The sensing response is found to increase almost linearly from 2.6 to 25.3 with an increase in H_2S gas concentration from 10 to 100 ppm, indicating the applicability of the sensor for the detection of concentration in real world applications. In addition, the well-ordered Cu-doped SnO_2 porous thin film sensor exhibits obvious advantages over the disordered porous thin film sensor. The disordered porous Cu-doped SnO_2 film was fabricated by using a mixture of PS beads with different diameters as the soft template. The sensitivity of the disordered sample to the concentration of H_2S that varied from 10 to 100 ppm at 180 °C is shown in Figure 6S of the Supporting Information. The well-ordered sample (in Figure 3b) presents a sensitivity (nearly 5 times) much higher than that of the disorder sample probably because of the much larger

specific surface area of the well-ordered sample. Furthermore, the well-ordered porous film sensor exhibits high reproducibility because of the uniform morphology and accurately controlled process, which is critical for practical industrial applications.

Selectivity is an important parameter of a sensing material in practical applications. Interference gases (methanol, acetone, ethanol, and carbon monoxide at 100 ppm) were used to investigate the selectivity of the undoped and Cu-doped SnO_2 porous thin film gas sensors to H_2S under the same condition, and the response to different gases is shown in Figure 4a. Only the Cu-doped SnO_2 sensor exhibits high selectivity toward the H_2S gas, with other interfering gases yielding a negligible response, while the undoped SnO_2 sensor shows similar responses to all the gases. The sensing mechanism of CuS formation in the Cu-doped SnO_2 sensor can explain the high selectivity of the Cu-doped SnO_2 sensor. In addition, the response times of the Cu-doped SnO_2 sample to the different testing gases are summarized in Figure 4b. It is noted that the Cu-doped SnO_2 porous film sensor shows the shortest response time to H_2S compared to the other interfering gases.

The long-term stability of the semiconductor gas sensor is also critical to its practical application. The sensitivity of Cu-doped SnO_2 porous thin film gas sensors to H_2S has been followed during the testing period as shown in Figure 5. It can

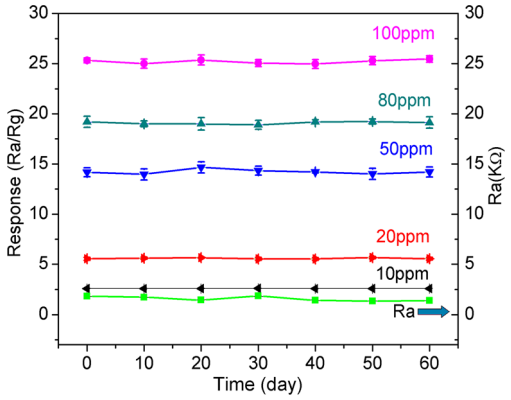

Figure 5. Long-term stability testing curve of Cu-doped SnO_2 gas sensors with respect to different concentrations of H_2S and R_a values of sensors at 180 °C.

be seen that the sensors exhibit a nearly constant response to H_2S at different concentrations (10, 20, 50, 80, and 100 ppm) over 60 days. Compared with those of the other H_2S gas sensors in the literature, for instance, SnO_2-based film sensors,[30] the sensing performance of the Cu-doped SnO_2 porous thin film sensors in this work with respect to H_2S has been improved dramatically. Besides, all the sensors fabricated with the soft template combined with the simple sputtering method developed in this work show good reproducibility in their sensing performance, which benefits from the well-defined porous nanostructure with a homogeneous and controllable film thickness and the pore size achieved by the rational fabrication process with easily controllable process parameters for fabricating the sensors in a highly reproducible yield.

CONCLUSION

In summary, we have developed a method combining the soft template and sputtering deposition for successfully fabricating well-ordered porous metal oxide semiconductor thin films for practical gas sensing applications. The well-defined Cu-doped SnO_2 porous thin film nanostructures with homogeneous and controllable film thickness and pore size have been fabricated for H_2S detection. The Cu-doped SnO_2 porous thin film sensor shows excellent sensing performance, including high sensitivity, selectivity, reproducibility, and short response and recovery time. The Cu-doped SnO_2 porous sensor has an optimal operating temperature of 180 °C, and the average response and recovery times with respect to 100 ppm of H_2S are ~10.1 and ~42.4 s, respectively. The Cu-doped SnO_2 sensor shows sensitivity 1 order of magnitude higher than that of and selectivity better than that of the undoped SnO_2 sensor because of the CuO−CuS conversion mechanism. The sensing response is found to increase almost linearly from 2.6 to 25.3 with an increase in H_2S gas concentration from 10 to 100 ppm. Importantly, the well-defined porous sensors fabricated by the facile method exhibit high reproducibility because of the accurately controlled process. The results demonstrate that the fabrication of controllable porous doped films is promising because of the low cost, low rate of power consumption, and high-performance gas sensor for H_2S, which can be easily extended to the fabrication of general semiconductor oxide gas sensors with easy doping and multilayer porous nanostructure.

ASSOCIATED CONTENT

Supporting Information

XRD and XPS results for undoped and Cu-doped SnO_2 porous thin films. This material is available free of charge via the Internet at http://pubs.acs.org.

AUTHOR INFORMATION

Corresponding Author

*E-mail: xhsun@suda.edu.cn. Fax: 86-512-65880820. Telephone: 86-512-65880943.

Notes

The authors declare no competing financial interest.

ACKNOWLEDGMENTS

The work was supported by the National Basic Research Program of China (973 Program) (Grant 2010CB934500), the Natural Science Foundation of China (NSFC) (Grant 91333112), and the Priority Academic Program Development of Jiangsu Higher Education Institutions. This project was also supported by the Fund for Innovative Research Teams of Jiangsu Higher Education Institutions.

REFERENCES

(1) Harrison, R.; Webb, J. A Review of the Effect of N Fertilizer Type on Gaseous Emissions. *Adv. Agron.* **2001**, *73*, 65−108.

(2) Mai, L.; Xu, L.; Gao, Q.; Han, C.; Hu, B.; Pi, Y. Single β-$AgVO_3$ Nanowire H_2S Sensor. *Nano Lett.* **2010**, *10* (7), 2604−2608.

(3) Lemieux, P. M.; Lutes, C. C.; Santoianni, D. A. Emissions of Organic Air Toxics from Open Burning: A Comprehensive Review. *Prog. Energy Combust. Sci.* **2004**, *30* (1), 1−32.

(4) Butnar, I.; Llop, M. Composition of Greenhouse Gas Emissions in Spain: An Input−Output Analysis. *Ecol. Econ.* **2007**, *61* (2−3), 388−395.

(5) Collins, P. G.; Bradley, K.; Ishigami, M.; Zettl, A. Extreme Oxygen Sensitivity of Electronic Properties of Carbon Nanotubes. *Science* **2000**, *287* (5459), 1801−1804.

(6) Modi, A.; Koratkar, N.; Lass, E.; Wei, B.; Ajayan, P. M. Miniaturized Gas Ionization Sensors Using Carbon Nanotubes. *Nature* **2003**, *424* (6945), 171−174.

(7) Péres, L. O.; Li, R. W. C.; Yamauchi, E. Y.; Lippi, R.; Gruber, J. Conductive Polymer Gas Sensor for Quantitative Detection of Methanol in Brazilian Sugar-Cane Spirit. *Food Chem.* **2012**, *130* (4), 1105−1107.
(8) Gourine, A. V.; Llaudet, E.; Dale, N.; Spyer, K. M. ATP is a Mediator of Chemosensory Transduction in the Central Nervous System. *Nature* **2005**, *436* (7047), 108−111.
(9) Rock, F.; Barsan, N.; Weimar, U. Electronic Nose: Current Status and Future Trends. *Chem. Rev.* **2008**, *108* (2), 705−725.
(10) Zhao, D.; Tan, S. W.; Yuan, D. Q.; Lu, W. G.; Rezenom, Y. H.; Jiang, H. L.; Wang, L. Q.; Zhou, H. C. Surface Functionalization of Porous Coordination Nanocages Via Click Chemistry and Their Application in Drug Delivery. *Adv. Mater.* **2011**, *23* (1), 90−93.
(11) Korotcenkov, G. Gas Response Control Through Structural and Chemical Modification of Metal Oxide Films: State of the Art and Approaches. *Sens. Actuators, B* **2005**, *107* (1), 209−232.
(12) Wu, N. L.; Wang, S. Y.; Rusakova, I. A. Inhibition of Crystallite Growth in the Sol-Gel Synthesis of Nanocrystalline Metal Oxides. *Science* **1999**, *285* (5432), 1375−1377.
(13) Sahm, T.; Mädler, L.; Gurlo, A.; Barsan, N.; Pratsinis, S. E.; Weimar, U. Flame Spray Synthesis of Tin Dioxide Nanoparticles for Gas Sensing. *Sens. Actuators, B* **2004**, *98* (2−3), 148−153.
(14) Occupational Safety and Health Administration (OSHA). Fact Sheet of Hydrogen Sulfide (H_2S), DSG, 2005.
(15) Hwang, I.-S.; Choi, J.-K.; Kim, S.-J.; Dong, K.-Y.; Kwon, J.-H.; Ju, B.-K.; Lee, J.-H. Enhanced H_2S Sensing Characteristics of SnO_2 Nanowires Functionalized with CuO. *Sens. Actuators, B* **2009**, *142* (1), 105−110.
(16) Verma, M.; Chowdhuri, A.; Sreenivas, K.; Gupta, V. Comparison of H_2S Sensing Response of Hetero-Structure Sensor (CuO-SnO_2) Prepared by Rf Sputtering and Pulsed Laser Deposition. *Thin Solid Films* **2010**, *518* (24), E181−E182.
(17) Khanna, A.; Kumar, R.; Bhatti, S. S. CuO-doped SnO_2 Thin Films as Hydrogen Sulphide Gas Sensor. *Appl. Phys. Lett.* **2003**, *82* (24), 4388−4390.
(18) Katti, V. R.; Debnath, A. K.; Muthe, K. P.; Kaur, M.; Dua, A. K.; Gadkari, S. C.; Gupta, S. K.; Sahni, V. C. Mechanism of Drifts in H_2S Sensing Properties of SnO_2: CuO Composite Thin Film Sensors Prepared by Thermal Evaporation. *Sens. Actuators, B* **2003**, *96* (1−2), 245−252.
(19) Xu, Z.; Duan, G.; Li, Y.; Liu, G.; Zhang, H.; Dai, Z.; Cai, W. CuO−ZnO Micro/Nanoporous Array-Film-Based Chemosensors: New Sensing Properties to H_2S. *Chem.—Eur. J.* **2014**, *20* (20), 6040−6046.
(20) Vasiliev, R. B.; Rumyantseva, M. N.; Yakovlev, N. V.; Gaskov, A. M. CuO/SnO_2 Thin Film Heterostructures as Chemical Sensors to H_2S. *Sens. Actuators, B* **1998**, *50* (3), 186−193.
(21) Kumar, V.; Sen, S.; Muthe, K. P.; Gaur, N. K.; Gupta, S. K.; Yakhmi, J. V. Copper Doped SnO_2 Nanowires as Highly Sensitive H_2S Gas Sensor. *Sens. Actuators, B* **2009**, *138* (2), 587−590.
(22) Patil, L. A.; Patil, D. R. Heterocontact Type CuO-Modified SnO_2 Sensor for the Detection of a ppm Level H_2S Gas at Room Temperature. *Sens. Actuators, B* **2006**, *120* (1), 316−323.
(23) Niranjan, R. S.; Chaudhary, V. A.; Mulla, I. S.; Vijayamohanan, K. A Novel Hydrogen Sulfide Room Temperature Sensor Based on Copper Nanocluster Functionalized Tin Oxide Thin Films. *Sens. Actuators, B* **2002**, *85* (1−2), 26−32.
(24) Singh, S.; Verma, N.; Singh, A.; Yadav, B. C. Synthesis and Characterization of CuO-SnO_2 Nanocomposite and Its Application as Liquefied Petroleum Gas Sensor. *Mater. Sci. Semicond. Process.* **2014**, *18*, 88−96.
(25) Chowdhuri, A.; Singh, S. K.; Sreenivas, K.; Gupta, V. Contribution of Adsorbed Oxygen and Interfacial Space Charge for Enhanced Response of SnO_2 Sensors Having CuO Catalyst for H_2S Gas. *Sens. Actuators, B* **2010**, *145* (1), 155−166.
(26) Tang, A. W.; Qu, S. C.; Li, K.; Hou, Y. B.; Teng, F.; Cao, J.; Wang, Y. S.; Wang, Z. G. One-pot Synthesis and Self-Assembly of Colloidal Copper(I) Sulfide Nanocrystals. *Nanotechnology* **2010**, *21*, 285602.
(27) Zhang, T.; Zeng, Y.; Fan, H. T.; Wang, L. J.; Wang, R.; Fu, W. Y.; Yang, H. B. Synthesis, Optical and Gas Sensitive Properties of Large-Scale Aggregative Flowerlike ZnO Nanostructures via Simple Route Hydrothermal Process. *J. Phys. D: Appl. Phys.* **2009**, *42*, 045103.
(28) Lim, S. K.; Hwang, S. H.; Chang, D.; Kim, S. Preparation of Mesoporous In_2O_3 Nanofibers by Electrospinning and Their Application as a CO Gas Sensor. *Sens. Actuators, B* **2010**, *149* (1), 28−33.
(29) Xue, X.; Xing, L.; Chen, Y.; Shi, S.; Wang, Y.; Wang, T. Synthesis and H_2S Sensing Properties of CuO−SnO_2 Core/Shell PN-Junction Nanorods. *J. Phys. Chem. C* **2008**, *112* (32), 12157−12160.
(30) Kumar, R.; Khanna, A.; Tripathi, P.; Nandedkar, R. V.; Potdar, S. R.; Chaudhari, S. M.; Bhatti, S. S. CuO-SnO_2 Element as Hydrogen Sulfide Gas Sensor Prepared by a Sequential Electron Beam Evaporation Technique. *J. Phys. D: Appl. Phys.* **2003**, *36* (19), 2377−2381.